

Electronic Supporting Information

A Near-infrared organic photosensitizer for use in dye-sensitized photoelectrochemical water splitting

Okta Suryani,^a Yuta Higashino,^a Jacob Yan Mulyana,^{*ab} Masayoshi Kaneko,^c Takayuki Hoshi,^c Koichiro Shigaki^c
and Yuji Kubo^{*ab}

^a*Department of Applied Chemistry, Graduate School of Urban Environmental Sciences, Tokyo Metropolitan University, 1-1 Minami-ohsawa, Hachioji, Tokyo 192-0397, Japan*

^b*Research Center for Hydrogen Energy Society, Tokyo Metropolitan University, Japan*

^c*Nippon Kayaku Co., Ltd., 31-12, Shimo 3-Chome, Kita-ku, Tokyo, 115-8588, Japan*

E-mail: ymulyana@tmu.ac.jp and yujik@tmu.ac.jp

Table of Contents

1. General	S2
2. Materials	S2
3. Synthesis of D1	S2
4. Photoanodes preparation	S5
5. Electrochemistry and photoelectrochemistry	S5
6. IPCE measurements	S5
7. Gas analysis	S5
8. Hydrogen peroxide analysis	S6
9. Faradaic efficiency, TON and TOF calculations	S6
10. Theoretical calculation	S6
11. References	S6
12. Scheme S1 Synthetic route to D1	S2
13. Fig. S1 Cyclic voltammogram of D1 in solution and FTO/TiO ₂ / D1 film	S7
14. Fig. S2 Absorption and fluorescence spectra of D1 in THF solution	S7
15. Fig. S3 Absorption spectra of D1 and C1 in solution before and after deposition	S8
16. Fig. S4 A photograph of the custom-made DSPEC compartment	S8
17. Fig. S5 Gas chromatogram of H ₂ in the gas sample	S9
18. Fig. S6 Gas chromatogram of O ₂ in the gas sample	S9
19. Fig. S7 Hydrogen peroxide analysis	S10
20. Fig. S8 Linear sweep voltammogram of FTO/TiO ₂ / D1 under on/off illumination	S10
21. Fig. S9 Cyclic voltammogram and photocurrent profile of FTO/TiO ₂ / D2-C1	S11
22. Fig. S10 Photographs of DSPEC cell showing the electrolyte solution after photolysis	S11
23. Fig. S11 ¹ H NMR spectrum of D1	S12
24. Fig. S12 ¹³ C NMR spectrum of D1	S13
25. Fig. S13 ¹¹ B NMR spectrum of D1	S14
26. Fig. S14 ¹⁹ F NMR spectrum of D1	S15
27. Fig. S15 ESI mass spectrum of D1	S16
28. Fig. S16 ¹ H NMR spectrum of C1	S17
29. Fig. S17 ESI mass spectrum of C1	S18

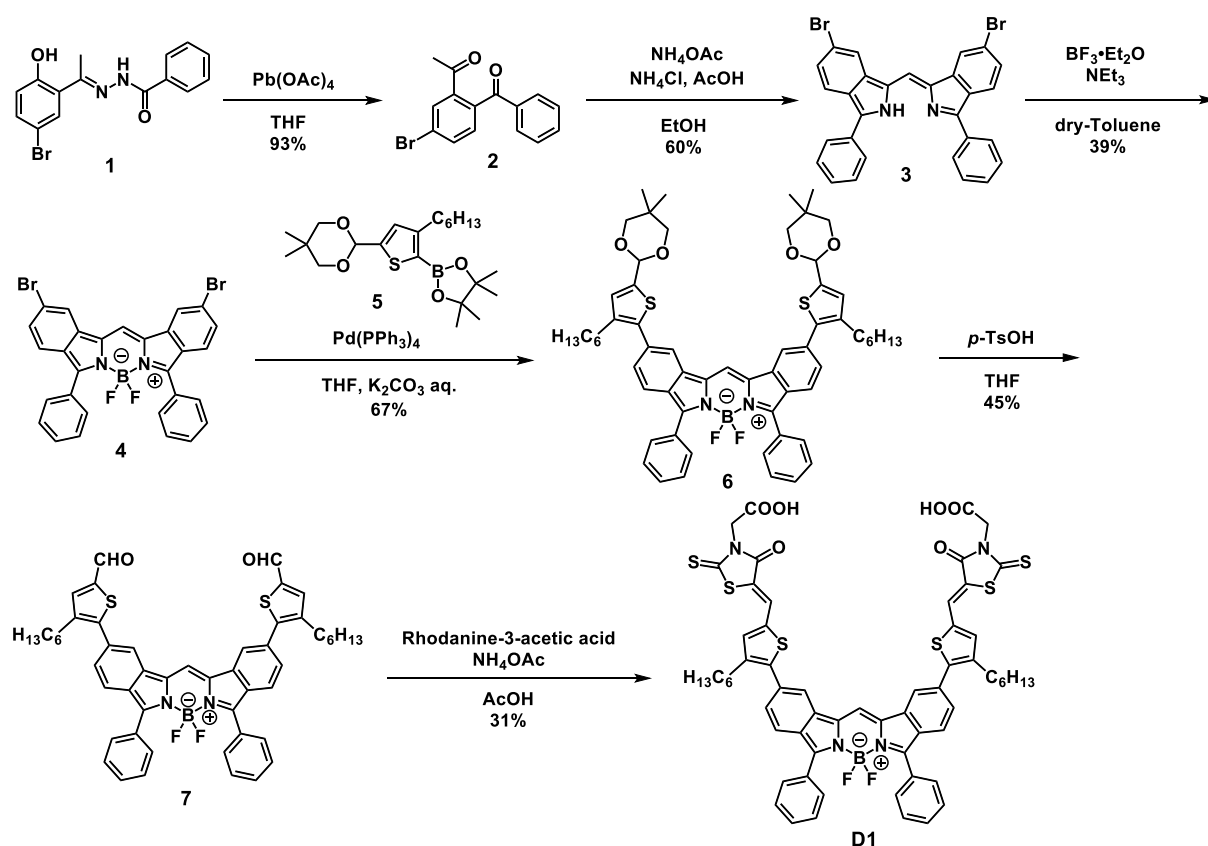
1. General

NMR spectra were measured on a Bruker Avance 500 MHz spectrometer (^1H : 500 MHz, ^{13}C : 125 MHz, ^{11}B : 160 MHz, ^{19}F : 470 MHz). In ^1H and ^{13}C NMR measurements are reported downfield from the internal standard Me_4Si . External standard for ^{19}F NMR and ^{11}B NMR were C_6F_6 and $\text{BF}_3\cdot\text{Et}_2\text{O}$ respectively. In addition, fast atom bombardment (FAB) mass spectra were obtained on JEOL JMS-700 where *m*-nitrobenzylalcohol was used as a matrix. Mass spectrometry data of compound **6** was taken by using electrospray ionization (ESI) method. The absorption and fluorescence spectra were measured using a Shimadzu UV-3600 and a JASCO FP-6300 spectrofluorometer, respectively. Elemental analysis was performed on an Exeter Analytical, Inc. CE-440F Elemental Analyser.

2. Materials

All chemicals and solvents used for the synthesis, if not otherwise stated, were commercially available and used as supplied. Dry toluene and dry THF were prepared according to the standard procedure. As for synthesis of **D1** (Scheme S1), 2-[1-(5-bromo-2-hydroxyphenyl)ethylidene]hydrazide **1**¹ and 2-(5-(5,5-dimethyl-1,3-dioxan-2-yl)-3-hexylthiophen-2-yl)-4,4,5,5-tetramethyl-1,3,2-dioxaborolane **5**² were conducted according to methods reported previously. Triphenyl amine dye **D2** was supplied by Nippon Kayaku Co. Ltd.. Ruthenium complex **C1** was synthesized according to the procedure reported earlier with slight modification.³

3. Synthesis



Scheme S1 Synthetic route to **D1**

l-(2-Benzoyl-5-bromophenyl)ethan-1-one (**2**). Pb(OAc)₄ (16.8 g, 37.8 mmol) was added into a solution of compound **1** (10.4 g, 31.5 mmol) in THF (540 mL) under an icy condition. The resulting mixture was stirred for 2h at room temperature. The resulting mixture was treated by filtration with silica gel to remove the remaining Pb(OAc)₄, and the solvent was finally removed by rotary evaporator to afford solid **2** (8.97 g, 93 % yield).

¹H NMR (500 MHz, CDCl₃): δ (ppm) 2.50 (s, 3H), 7.30 (d, 1H, *J* = 8.15 Hz), 7.43 (tt, 2H, *J* = 7.70 and 1.57 Hz), 7.56 (tt, 1H, *J* = 7.43 Hz and 1.45 Hz), 7.72 (dt, 2H, *J* = 6.85 Hz and 1.55 Hz), 7.75 (dd, 1H, *J* = 8.10 and 1.90 Hz), 7.96 (d, 1H, *J* = 1.90 Hz). FAB-MS: *m/z* = 301[M]⁺

(*Z*)-6-Bromo-1-((6-bromo-3-phenyl-2*H*-isoindol-1-yl)methylene)-3-phenyl-1*H*-isoindole (**3**). Acetic acid (77 mL) was added into a solution of compound **2** (8.97 g, 29.6 mmol) in ethanol (385 ml) at room temperature, followed by the addition of NH₄OAc (13.7 g, 178 mmol) and NH₄Cl (1.58 g, 29.6 mmol) at 65 °C. The resulting mixture was stirred at 90 °C for 5 h. Upon completion, the mixture was poured dropwise into saturated NaHCO₃ aqueous solution (571 mL). The collected precipitate was chromatographed on silica gel with CH₂Cl₂/hexane (1:3 v/v) and recrystallized using CH₂Cl₂/methanol to give 4.91 g of compound **3** in 60% yield.

¹H NMR (500 MHz, CDCl₃): δ (ppm) 7.37 (dd, 2H, *J* = 8.55 and 1.70 Hz), 7.45 (s, 1H), 7.48 (tt, 2H, *J* = 7.40 and 1.41 Hz), 7.57 (t, 4H, *J* = 7.65 Hz), 7.86 (d, 2H, *J* = 8.65 Hz), 7.98 (dd, 4H, *J* = 8.15 and 1.00 Hz), 8.04 (d, 2H, *J* = 1.25 Hz). ¹³C NMR (125 MHz, CDCl₃): δ (ppm) 147.3, 137.4, 133.2, 132.3, 129.2, 129.1, 128.1, 127.6, 127.5, 123.4, 122.1, 121.2, 112.4, 77.63. FAB-MS: *m/z* = 553[M]⁺

Difluoro[6-bromo-1-[[6-bromo-3-phenyl-2*H*-isoindole-1-yl]methylene]-3-phenyl-1*H*-isoindolate-*N*¹,*N*²]boron (**4**). Under N₂ condition, compound **3** (1.91 g, 3.45 mmol) was dissolved in toluene (140 mL) followed by the addition of NEt₃ (0.70 mL, 0.505 mmol). After adding BF₃·Et₂O (4.5 mL, 35.8 mmol) to the mixture at 80 °C, the resulting mixture was stirred for 3 h at 100 °C. The resulting mixture was poured into water and extracted by CH₂Cl₂, the organic layer was washed with water and dried by Na₂SO₄. After removing the solvent, the solid was collected to give 0.806 g of compound **5** with 39% yield.

¹H NMR (500 MHz, CDCl₃): δ (ppm) 7.34 (dd, 2H, *J* = 8.72 and 1.62 Hz), 7.46 – 7.52 (m, 8H), 7.77 (dd, 4H, *J* = 8.15 and 1.55 Hz), 7.78 (s, 1H), 8.06 (dd, 2H, *J* = 1.50 and 0.50 Hz). ¹³C NMR (125 MHz, CDCl₃): δ (ppm) 152.3, 135.2, 130.0, 129.9, 129.1, 128.8, 128.3, 126.8, 125.2, 124.3, 121.8, 115.2, 77.6. HRMS (FAB): *m/z* [M]⁺ calcd for C₂₉H₁₇BBF₂N₂, 599.9820; found, 599.9810.

Difluoro[6-(3-hexyl-5-(5,5-dimethyl-[1,3]dioxane-2-yl)thiophen-2-yl)-1-[[6-(3-hexyl-5-(5,5-dimethyl-[1,3]dioxane)thiophene-2-yl)-3-phenyl-2*H*-isoindole-1-yl]methylene]-3-phenyl-1*H*-isoindolate-*N*¹,*N*²]boron (**6**). Compound **4** (1.20 g, 1.99 mmol) and **5** (2.50 g, 6.12 mmol) were dissolved in THF (96 mL), followed by the addition of 2M K₂CO₃ aq. (19.7 mL). The resulting mixture was degassed by freeze-pump-thaw cycles. Upon the addition of Pd(PPh₃)₄ (0.5 g, 0.433 mmol) into the frozen flask under nitrogen, the mixture was stirred overnight at 70 °C. The resulting mixture was poured into water and extracted by AcOEt. The organic layer was washed with water and dried by Na₂SO₄. After the removal of the solvent in vacuo, the residue was chromatographed on silica gel with CH₂Cl₂/hexane (1:1, v/v) as an eluent to afford compound **6** (1.34 g, 67%).

¹H NMR (500MHz, CDCl₃): δ (ppm) 0.819 (s, 12H), 1.25 (sextet, 4H, *J* = 3.68 Hz), 1.29 – 1.32 (m, 8H), 1.31 (t, 6H, *J* = 6.22 Hz), 1.63 (q, 4H, *J* = 7.63 Hz), 2.70 (t, 4H, *J* = 7.82 Hz), 3.67 (d, 4H, *J* = 10.8 Hz), 3.79 (d, 4H, *J* = 11.3 Hz), 5.64 (s, 2H), 7.08 (s, 2H), 7.32 (dd, 2H, *J* = 8.47 and 1.48 Hz), 7.45 – 7.52 (m, 6H), 7.63 (dd, 2H, *J* = 8.42 and 0.63 Hz), 7.80 (s, 1H), 7.83 (dd, 4H, *J* = 7.93 and 1.42 Hz), 7.93 – 7.94 (m, 2H). ¹³C NMR (125 MHz, CDCl₃): δ (ppm) 151.7, 140.0, 139.1, 137.9, 135.8, 134.7, 131.0, 130.2, 129.6, 128.3, 128.0, 127.7, 127.0, 123.7, 119.4, 114.4, 98.4, 77.6, 31.6, 30.9, 30.3, 29.7, 29.2, 29.0, 23.0, 22.6, 21.9, 14.1. HRMS (ESI): *m/z* [M+Na]⁺ calcd for C₆₀H₆₇BN₂O₄S₂F₂Na, 1027.4505; found, 1027.4484
HRMS (ESI): *m/z* [M+K]⁺ calcd for C₆₀H₆₇BN₂O₄S₂F₂K, 1043.4245; found, 1043.4240.

Difluoro[6-(3-hexyl-5-formylthiophene-2-yl)-1-[[6-(3-hexyl-5-formylthiophene-2-yl)-3-phenyl-2H-isoindole-1-yl]methylene]-3-phenyl-1H-isoindolate-N¹,N²]boron (7). Compound **6** (1.34 g, 1.33 mmol) was dissolved in THF (172 mL), followed by the addition of *p*-toluene sulfonic acid monohydrate (0.512 g, 2.69 mmol) in water (35.5 mL). The reaction mixture was stirred for 7 h at 40 °C. The resulting mixture was poured into water and extracted by AcOEt and the organic layer was washed with water and dried by Na₂SO₄. After the removal of the solvent, the residue was chromatographed on silica gel with CH₂Cl₂/hexane (3:2 v/v) as an eluent to give 0.498 g of compound **7** with 45% yield.

¹H NMR (500MHz, CDCl₃): δ (ppm) 0.838 (t, 6H, *J* = 6.98 Hz), 1.25 – 1.27 (m, 8H), 1.33 (q, 4H, *J* = 7.06 Hz), 1.66 (q, 4H, *J* = 7.59 Hz), 2.76 (t, 4H, *J* = 7.80 Hz), 7.32 (dd, 2H, *J* = 8.45 and 1.45 Hz), 7.48 – 7.53 (m, 6H), 7.70 (d, 2H, *J* = 9.70 Hz), 7.70 (s, 2H), 7.84 (dd, 4H, *J* = 7.67 and 1.77 Hz), 7.89 (s, 1H), 7.99 (s, 2H), 9.90 (s, 2H).
¹³C NMR (125 MHz, CDCl₃): δ (ppm) 182.8, 152.2, 148.1, 141.8, 141.1, 138.4, 134.5, 134.2, 130.6, 130.2, 129.9, 128.4, 128.1, 126.5, 124.2, 119.8, 114.8, 77.6, 31.6, 30.7, 29.0, 28.8, 22.6, 14.0. HRMS (FAB): *m/z* [M]⁺ calcd for C₅₁H₄₇BF₂N₂O₂S₂, 832.3140; found, 832.3145.

Difluoro[6-(3-hexyl-5-((3-carboxymethyl)-4-oxo-2-thioxothiazolidin-5-ylidene)methyl)thiophene-2-yl)-1-[[6-(3-hexyl-5-((3-carboxymethyl)-4-oxo-2-thioxothiazolidin-5-ylidene)methyl)thiophene-2-yl)-3-phenyl-2H-isoindole-1-yl]methylene]-3-phenyl-1H-isoindolate-N¹,N²]boron (D1). Under nitrogen atmosphere, a mixture of compound **7** (0.288 g, 0.35 mmol), rhodanine-3-acetic acid (0.225 g, 1.18 mmol) and NH₄OAc (0.138 g, 1.80 mmol) in CH₃COOH (10 mL) was stirred over night at 120 °C. The resulting mixture was poured into water (100 mL) resulting in the appearance of a brown solid. The solid product was collected by filtration and washed with water until pH 7. The crude product was chromatographed over silica gel using a gradient eluent MeOH in CH₂Cl₂ (0-100%) to afford 0.130 g of the product (31% yield).

¹H NMR (500MHz, THF-*d*₈): δ (ppm) 0.833 (t, 6H, *J* = 6.85 Hz), 1.27 – 1.29 (m, 12H), 1.32 – 1.37 (m, 4H), 2.86 (t, 4H, *J* = 7.62 Hz), 4.78 (s, 4H), 7.46 – 7.53 (m, 8H), 7.59 (s, 2H), 7.75 (d, 2H, *J* = 8.35 Hz), 7.86 (d, 4H, *J* = 6.75 Hz), 7.98 (s, 2H), 8.29 (s, 2H), 8.55 (s, 1H). ¹³C NMR (125 MHz, THF-*d*₈) δ (ppm): 204.8, 192.9, 167.3, 152.7, 147.2, 142.8, 138.7, 137.6, 135.6, 135.4, 131.9, 131.1, 130.4, 129.4, 129.0, 126.9, 126.1, 124.8, 121.5, 121.1, 45.7, 32.5, 31.5, 30.6, 30.4, 30.0, 29.6, 23.5, 14.4. ¹⁹F NMR (470 MHz, THF-*d*₈) δ (ppm): -129.6 (quartet, *J*_{BF} = 31.1 Hz). ¹¹B NMR (160 MHz, THF-*d*₈) δ (ppm): 3.98 (triplet, *J*_{FB} = 31.2 Hz). ESI-MS (negative mode): *m/z* = 1177[M-H]⁻. Elemental analysis: calcd for C₆₁H₅₃BF₂N₄O₆S₆·2H₂O: C, 60.28; H, 4.73; N, 4.61, found: C, 60.13; H 4.41; N 4.61%.

4. Photoanodes preparation

Transparent TiO₂ films of 9 mm × 9 mm size with 10 μm thickness printed on FTO glass was used for the deposition of the dyes. For the photoanodes fabrication, the corresponding dye solution (0.25 mM) in THF/acetone (1:9) was deposited for 20 hours followed by drying and immersing in the methanol solution of **C1** (0.20 mM) for 20 hours. The dye and catalyst loading was estimated by measuring the absorbance of the solution before and after the deposition, giving the mole of the deposited materials, which was then converted to the dye amount loaded on the TiO₂ in mol cm⁻², taking into account the film area 0.81 cm². The **D1**, **C1** and **D2** amounts loaded were calculated by this method to be 3.07×10^{-7} mol cm⁻², 0.609×10^{-7} mol cm⁻² and 3.24×10^{-7} mol/cm², respectively.

5. Electrochemistry and photoelectrochemistry

Electrochemical and photoelectrochemical measurements were performed on a Princeton Applied Research VersaSTAT 3 potentiostat that is connected to a personal computer for controlling the measurement using a VersaSTAT 3 software package. For electrochemistry in organic solvents, the experiments were performed on a typical three-electrode cell using glassy carbon working electrode, Ag/AgNO₃ reference electrode and Pt counter electrode. The potential values were converted to NHE scale using ferrocene as an internal reference ($E_{1/2}$ Fc = 0.63 V vs. NHE)⁴.

For electrochemistry and photoelectrochemistry involving the photoanode films, the measurements were performed on a custom-made glass cell, which has compartments for inserting electrodes as shown in Fig. S4. All experimental set up uses a three-electrode system with the corresponding photoanodes as working electrode, Ag/AgCl (3 M NaCl aqueous solution) as reference electrode and Pt wire as counter electrode. The potential values were converted to NHE ($E_{\text{NHE}} = E_{\text{Ag/AgCl}} + 0.207$ V)⁵. Nitrogen gas was purged into the DSPEC compartment for about 20 minutes prior to each measurement. Xenon lamp 300 W (Max-303 from Asahi Spectra Co., Ltd) with 400 nm long pass filter was used to irradiate the photoanode from the FTO side. The Xenon lamp is equipped with a light guide that can provide approximately 1 cm × 1 cm illumination area. The lamp has the adjustment setting to control the light power and a 200 mW cm⁻² light intensity, as measured by an ADCMT 8230E Optical Power Meter from ADC Corporation, was used to irradiate the photoanode sample.

6. IPCE measurements

For the IPCE measurements, FTO/TiO₂/**D1** and FTO/TiO₂/**D1-C1** working electrodes were fabricated in a device by combining with a platinized counter electrode and the insertion of a liquid electrolyte comprising of I₂ (0.1 M), LiI (0.1 M) and dimethylpropylimidazolium iodide (0.6 M) in methoxypropionitrile. The incident photon-to-charge carrier efficiencies (IPCEs) were measured on the IPCE Measurement System (SM-250, Bunkoukeiki Co., Ltd.).

7. Gas analysis

The gas sample was withdrawn from the DSPEC compartment through a septum using a VICI pressure lock precision gas syringe and injected to a Shimadzu GC2010 Gas Chromatograph equipped with a BID-2010 plus detector. A micropacked ST column was used to separate the gases at oven temperature 35 °C using helium gas carrier. Hydrogen and oxygen gases were calibrated and quantified using 5% H₂ in Ar and 5% O₂ in He reference gases, respectively, purchased from Taiyo Nippon Sanso Co., Ltd..

8. Hydrogen peroxide analysis

The analysis of hydrogen peroxide content in the electrolyte solution follows the procedure reported previously.⁶ The analysis was based on the stoichiometric reaction of H₂O₂ with Fe²⁺ to form OH⁻ and Fe³⁺ (H₂O₂ + Fe²⁺ → Fe³⁺ + 2OH⁻), which can be monitored spectroscopically. Thus, reacting FeSO₄ (0.05 M) standard solution in the mixture of H₂SO₄ (0.01 M) and phosphate buffer pH 5.8 (0.05 M) in the presence of increasing concentration of H₂O₂ gives the increasing absorbance at 295 nm corresponding to the formation of Fe³⁺ species (Fig. S7a). The plot of Δ(Abs) versus [H₂O₂] gives the straight line (Fig. S7b), which was used as the standard curve for the determination of the H₂O₂ concentration in the samples.

9. Faradaic efficiency, TON and TOF calculations

Faradaic efficiency of oxygen and hydrogen production was calculated according to the following equations:

$$\eta_{O_2} = \frac{4n_{O_2}}{Q} \quad (1)$$

$$\eta_{H_2} = \frac{2n_{H_2}}{Q} \quad (2)$$

where n_{O_2} and n_{H_2} are mole of each gas observed from the experiments and $Q = \text{Coulomb} / 96485$.

The TON values were calculated according to the equation $\text{TON} = n(O_2)$ after 2000 seconds / $n(\text{catalyst})$ loading 0.0493 μmol estimated from the absorbance of C1 before and after the deposition. The TOF was obtained from the equation $\text{TOF} = \text{TON}/t$ where $t = 33.3$ minutes (2000 seconds) (the duration of the photolysis).

10. Theoretical calculation

All geometries of D1 at the ground state were fully optimized by means of the B3LYP/6-31G(d,p) level method. Density functional theory (DFT) calculations at the B3LYP/6-31G(d,p) level were performed in the Gaussian 09 package.⁷ The molecular orbitals were visualized using the Gauss view 5.0.8 program.

11. References

1. C. Z. Zheng, L. Wang, J. Liu. *Adv. Mater. Res.*, 2011, **239-242**, 2153.
2. Y. Kubo, D. Eguchi, A. Matsumoto, R. Nishiyabu, H. Yakushiji, K. Shigaki, and M. Kaneko. *J. Mater. Chem. A*, 2014, **2**, 5204.
3. Y. Gao, L. Zhang, X. Ding, and L. Sun, *Phys. Chem. Chem. Phys.*, 2014, **16**, 12008.
4. T. Daeneke, A. J. Mozer, T-H. Kwon, N. W. Duffy, A. B. Holmes, U. Bach and L. Spiccia. *Energy Environ. Sci.*, 2012, **5**, 7090.
5. L. Alibabaei, M. K. Brennaman, M. R. Norris, B. Kalanyan, W. J. Song, M. D. Losego, J. J. Concepcion, R. A. Binstead, G. N. Parsons and T. J. Meyer, *Proc. Natl. Acad. Sci. USA*, 2013, **110**, 20008-20013.
6. M. Steiner and N. Lazaroff, *Applied Microbiology*, 1974, **28**, 872-880.
7. Frisch, M. J.; Trucks, G. W.; Schlegel, H. B.; Scuseria, G. E.; Robb, M. A.; Cheeseman, J. R.; Scalmani, G.; Barone, V.; Mennucci, B.; Petersson, G. A.; Nakatsuji, H.; Caricato, M. L., X.; Hratchian, H. P.; Izmaylov, A. F.; Bloino, J.; Zheng, G.; Sonnenberg, J. L.; Hada, M.; Ehara, M.; Toyota, K.; Fukuda, R.; Hasegawa, J.; Ishida, M.; Nakajima, T.; Honda, Y.; Kitao, O.; Nakai, H.; Vreven, T.; Montgomery, J. A.,

Jr.; Peralta, J. E.; Ogliaro, F.; Bearpark, M.; Heyd, J. J.; Brothers, E.; Kudin, K. N.; Staroverov, V. N.; Keith, T.; Kobayashi, R.; Normand, J.; Raghavachari, K.; Rendell, A.; Burant, J. C.; Iyengar, S. S.; Tomasi, J.; Cossi, M.; Rega, N.; Millam, J. M.; Klene, M.; Knox, J. E.; Cross, J. B.; Bakken, V.; Adamo, C.; Jaramillo, J.; Gomperts, R.; Stratmann, R. E.; Yazyev, O.; Austin, A. J.; Cammi, R.; Pomelli, C.; Ochterski, J. W.; Martin, R. L.; Morokuma, K.; Zakrzewski, V. G.; Voth, G. A. S., P.; Dannenberg, J. J.; Dapprich, S.; Daniels, A. D.; Farkas, O.; Foresman, J. B.; Ortiz, J. V.; Cioslowski, J.; Fox, D. J.; Gaussian, Inc: Wallingford, CT, 2010.

8. R. Zhu, C-Y. Jiang, B. Liu and S. Ramakrishna, *Adv. Mater.*, 2009, **21**, 994; M. Plannells, A. Abate, D. J. Hollman, S. D. Stranks, V. Bharti, J. Gaur, D. Mohanty, S. Chand, H. J. Snaith and N. Robertson, *J. Mater. Chem. A*, 2013, **1**, 6949.

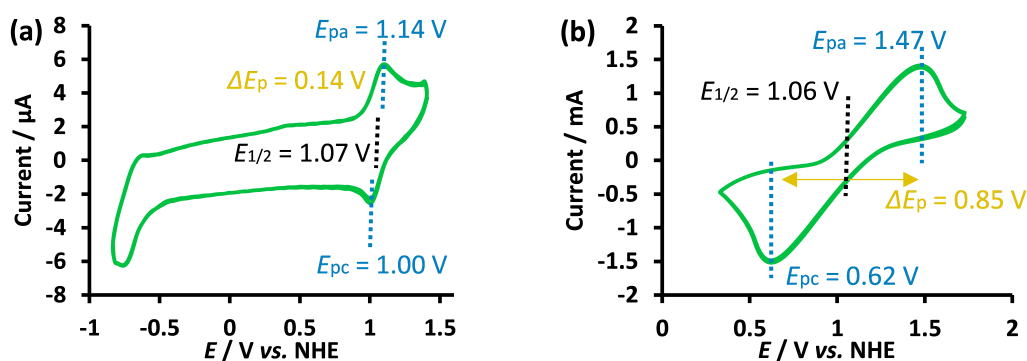


Fig. S1 (a) Cyclic voltammogram of **D1** (0.5 mM) in deaerated acetonitrile/*o*-dichlorobenzene (1:4) containing 0.1 M TBAPF₆ electrolyte; the anodic scan shows a reversible wave at the $E_{1/2}$ 1.07 V vs. NHE assigned to **D1**⁺/**D1**; (b) Cyclic voltammogram of FTO/TiO₂/**D1** in deaerated acetonitrile containing 0.1 M TBAPF₆ electrolyte showing the **D1**⁺/**D1** quasi-reversible wave at the mid-way potential $E_{1/2}$ 1.06 V vs. NHE. The scan rate was 0.1 V sec⁻¹. The larger ΔE_p value for **D1** in FTO/TiO₂/**D1** in comparison to the measurement in solution is consistent with the previous finding by Ramakhrisna and Robertson (ref. 8), which is presumably due to the slower kinetics of the electron transfer on the surface of TiO₂.

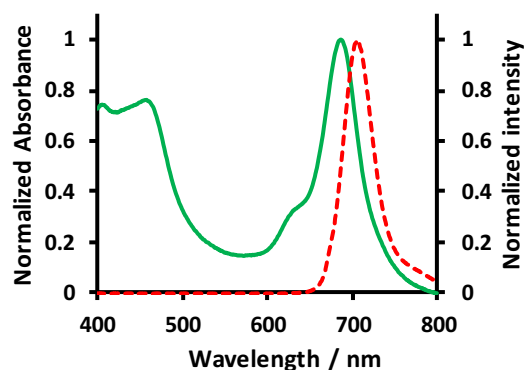


Fig. S2 Absorption (green) and fluorescence (red) spectra of **D1** in THF (1 μ M), showing the intersection at $\lambda = 698$ nm, which afforded the zeroth-zeroth transition energy E_{0-0} 1.78 eV.

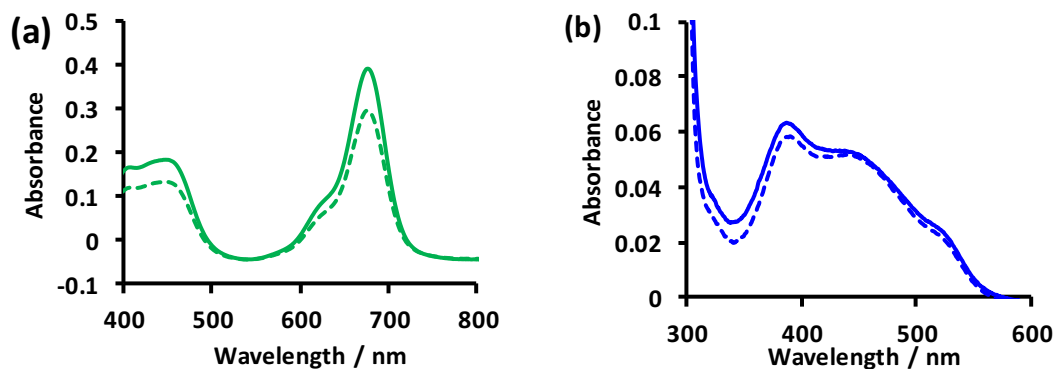


Fig. S3 Absorption spectra of (a) **D1** in THF/acetone (1:9) and (b) **C1** in methanol measured before (solid line) and after (dashed line) the film deposition. The decrease in the absorbance indicates the adsorption of the substances onto TiO_2 .

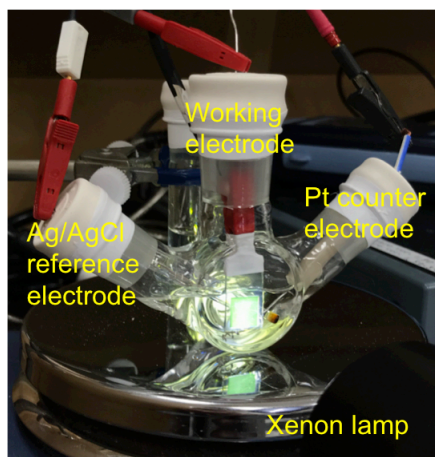


Fig. S4 A photograph of the custom-made DSPEC containing $\text{FTO}/\text{TiO}_2/\mathbf{D1-C1}$ working electrode, Ag/AgCl reference electrode and platinum counter electrode that are connected to a potentiostat. A Xenon lamp with a light guide was used to irradiate the photoanode from the FTO side.

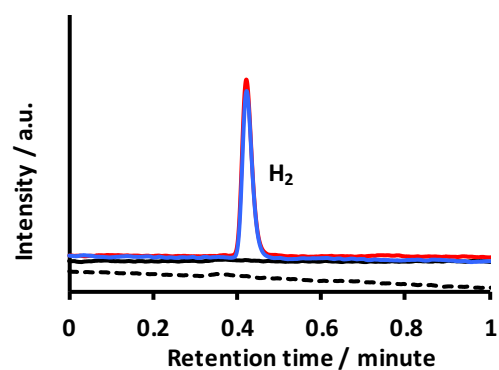


Fig. S5 Gas chromatograms showing the hydrogen peak at 0.4 min retention time taken after 2000-second photolysis of FTO/TiO₂/D1-C1 at pH 7.2 (red) and at pH 5.8 (blue). The black dashed line represents the chromatogram of the gas sample withdrawn from the headspace of the DSPEC compartment prior to the experiment. The black solid line represents the chromatogram of the air background, which was performed under the same condition using FTO/TiO₂ working electrode.

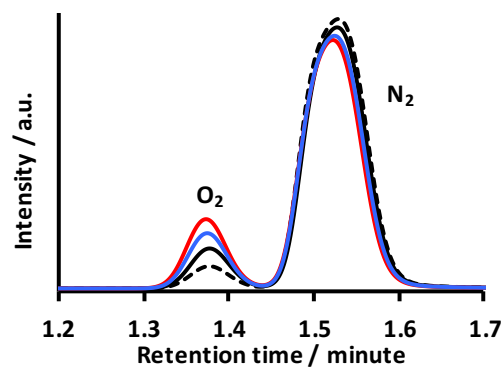


Fig. S6 Gas chromatograms showing the oxygen peak at 1.37 min retention time taken after 2000-second photolysis of FTO/TiO₂/D1-C1 at pH 7.2 (red) and at pH 5.8 (blue). The black dashed line represents the chromatogram of the gas sample withdrawn from the headspace of the DSPEC compartment prior to the experiment. The black solid line represents the chromatogram of the air background, which was performed under the same condition using FTO/TiO₂ working electrode.

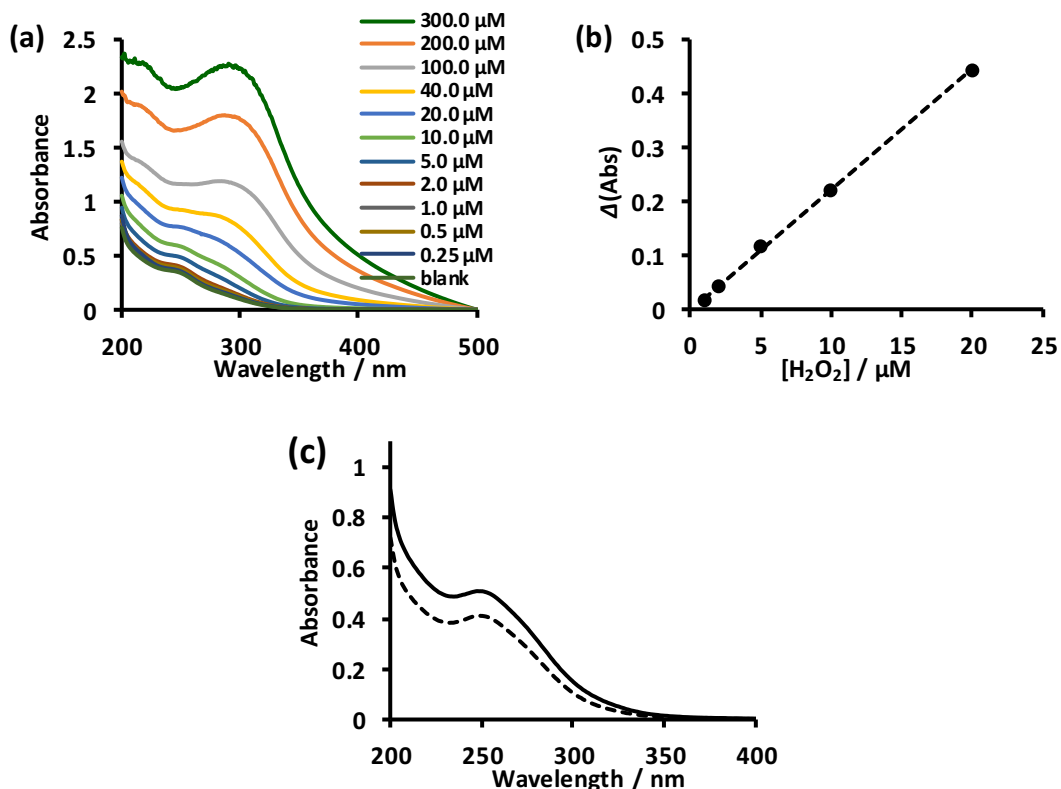


Fig. S7 (a) The progressive appearance of the absorbance at 295 nm upon increasing the H_2O_2 quantity that reacts with Fe^{2+} is indicative of the formation of Fe^{3+} ; (b) The standard curve was obtained from plotting the $\Delta(\text{Abs})$ versus the concentration of H_2O_2 ; (c) The absorption spectra of the electrolyte (phosphate buffer pH 5.8) reacted with FeSO_4 (black solid line) of the DSPEC compartment with $\text{FTO}/\text{TiO}_2/\mathbf{D1-C1}$ after photolysis in comparison with that of the blank (buffer solution before electrolysis + FeSO_4) given in dashed line. The $\Delta(\text{Abs})$ obtained from the data was fitted into the standard curve to obtain the mole of H_2O_2 in the sample.

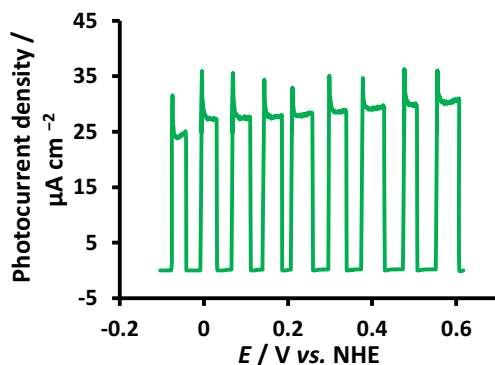


Fig. S8 Linear sweep voltammogram (LSV) of $\text{FTO}/\text{TiO}_2/\mathbf{D1}$ at pH 7.2 under on/off illumination taken between -0.1 and 0.6 V vs. NHE at the scan rate 0.005 V sec^{-1} . The good photocurrent response indicates the ability of photo-excited $\mathbf{D1}^*$ to inject electron to the conduction band of TiO_2 .

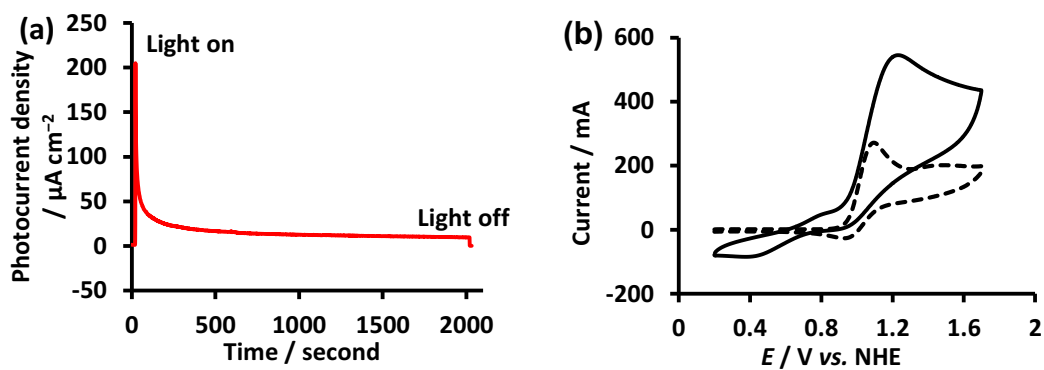


Fig. S9 (a) Photocurrent profile obtained during a 2000-second photolysis of FTO/TiO₂/D2-C1 at 0.207 V vs. NHE performed in 0.1 M NaF aqueous solution. (b) Cyclic voltammogram of FTO/TiO₂/D2-C1 (solid line) in comparison with FTO/TiO₂/D2 (dashed) obtained at pH 7.2. The dye's D2^{•+}/D2 in FTO/TiO₂/D2 is apparent at 1.0 V vs. NHE, which moves slightly to 1.1 V vs. NHE in FTO/TiO₂/D2-C1. Despite the presence of Ru^{III}/Ru^{II} at 0.6 V vs. NHE and the increase in the E_{pa} of D2^{•+}/D2 as a result of the co-deposition with C1, the peak for Ru^{IV}/Ru^{III} is not observed clearly.

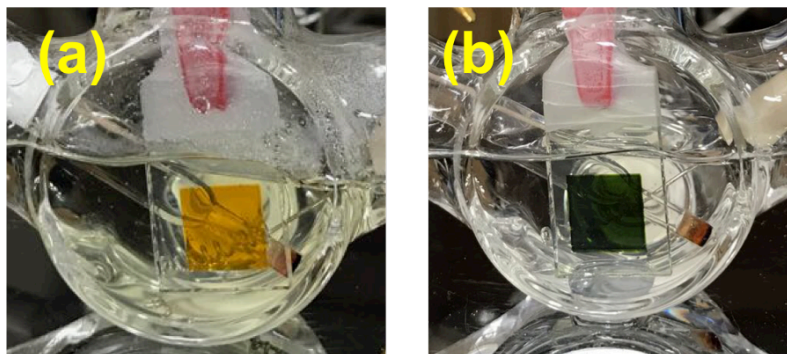


Fig. S10 (a) The photograph of the DSPEC compartment with FTO/TiO₂/D2-C1 after 2000-second photolysis showing the coloration of the electrolyte, indicative of the detachment of D2 from TiO₂ in contrast to the clear solution obtained after the photolysis of FTO/TiO₂/D1-C1 (b), which suggests that that D1 remains intact in TiO₂ during the course of the photolysis.

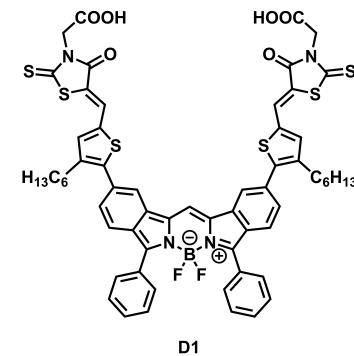
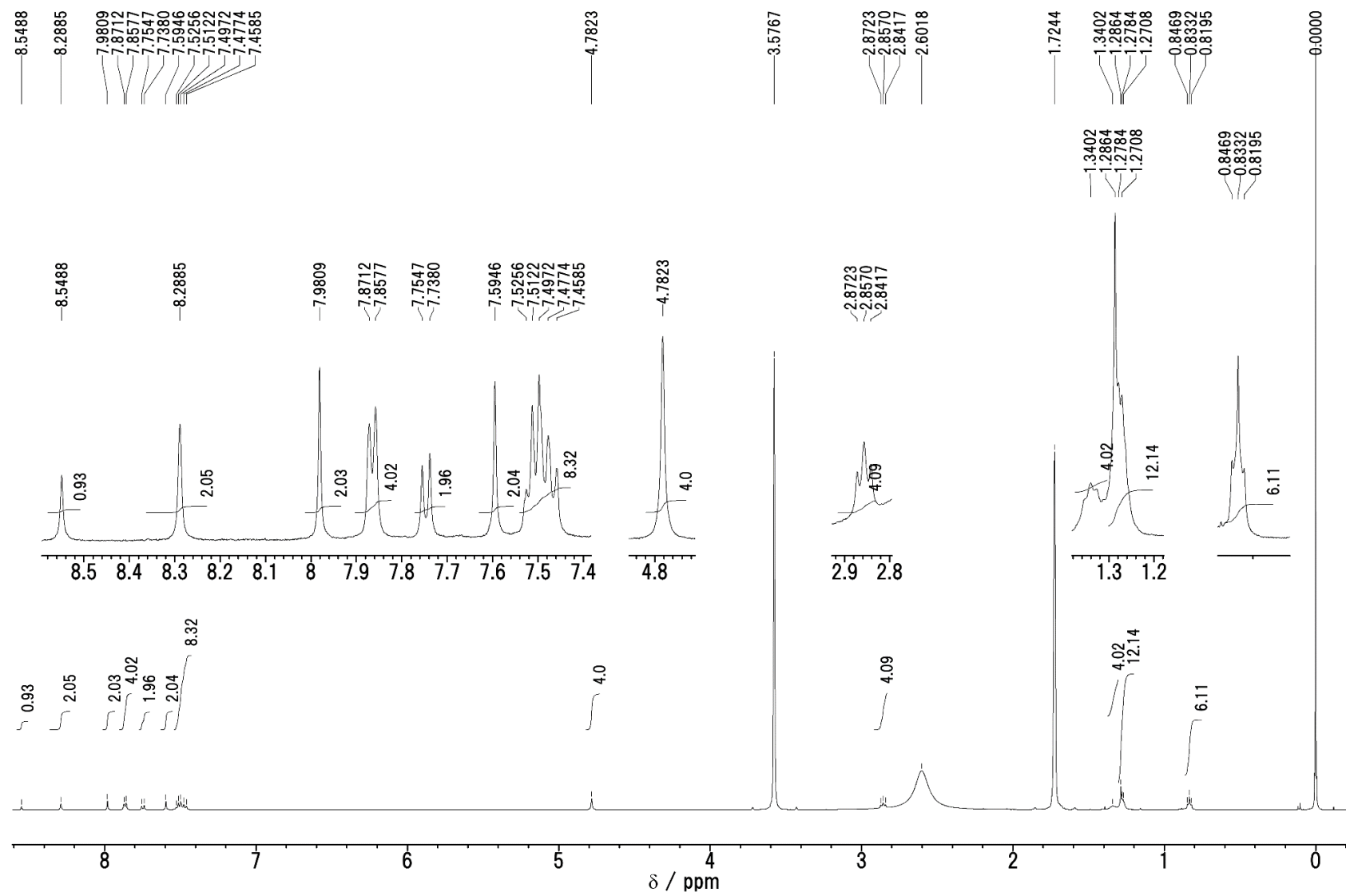


Fig. S11 ^1H NMR spectrum of D1

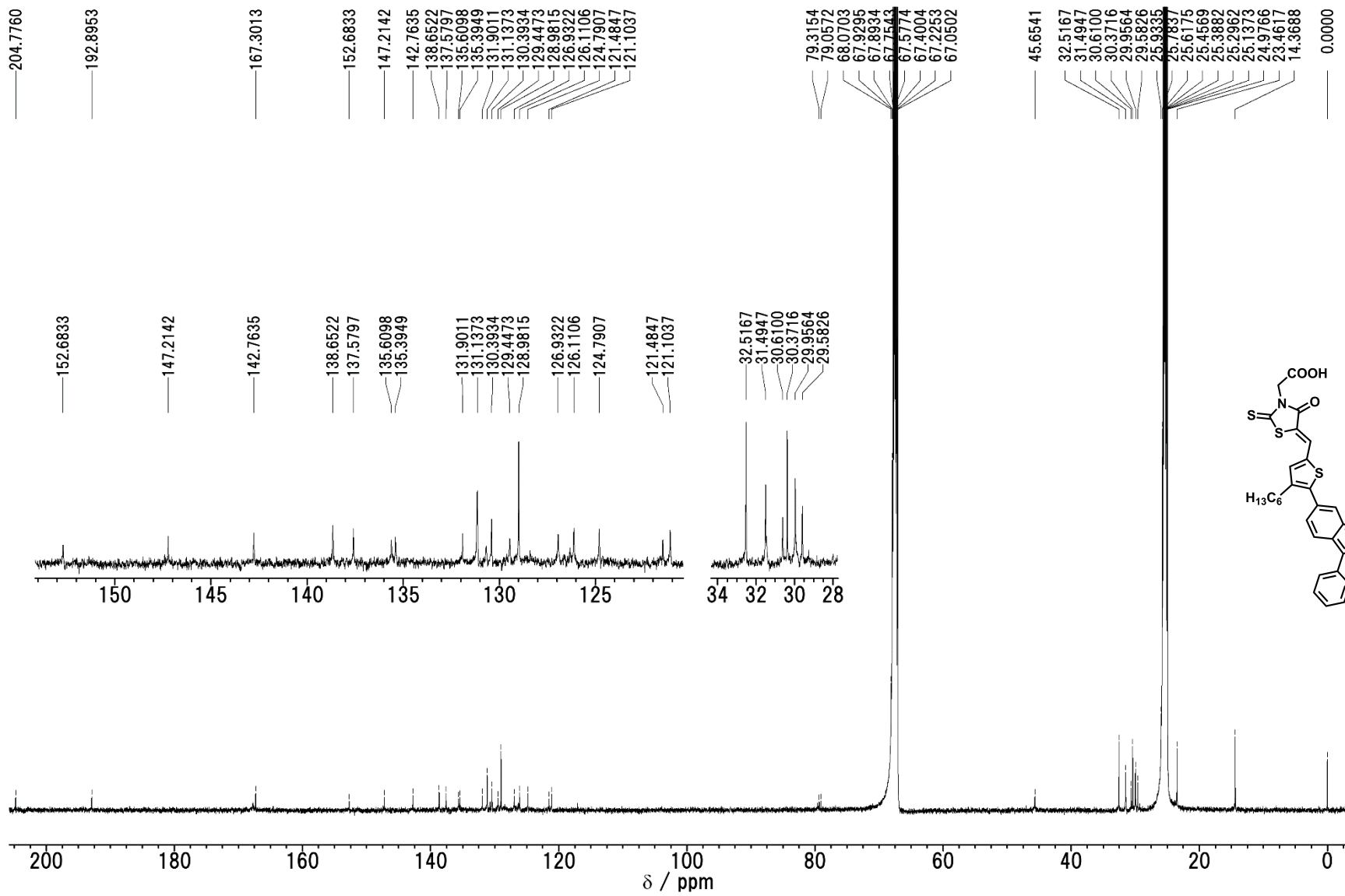


Fig. S12 ^{13}C NMR spectrum of D1

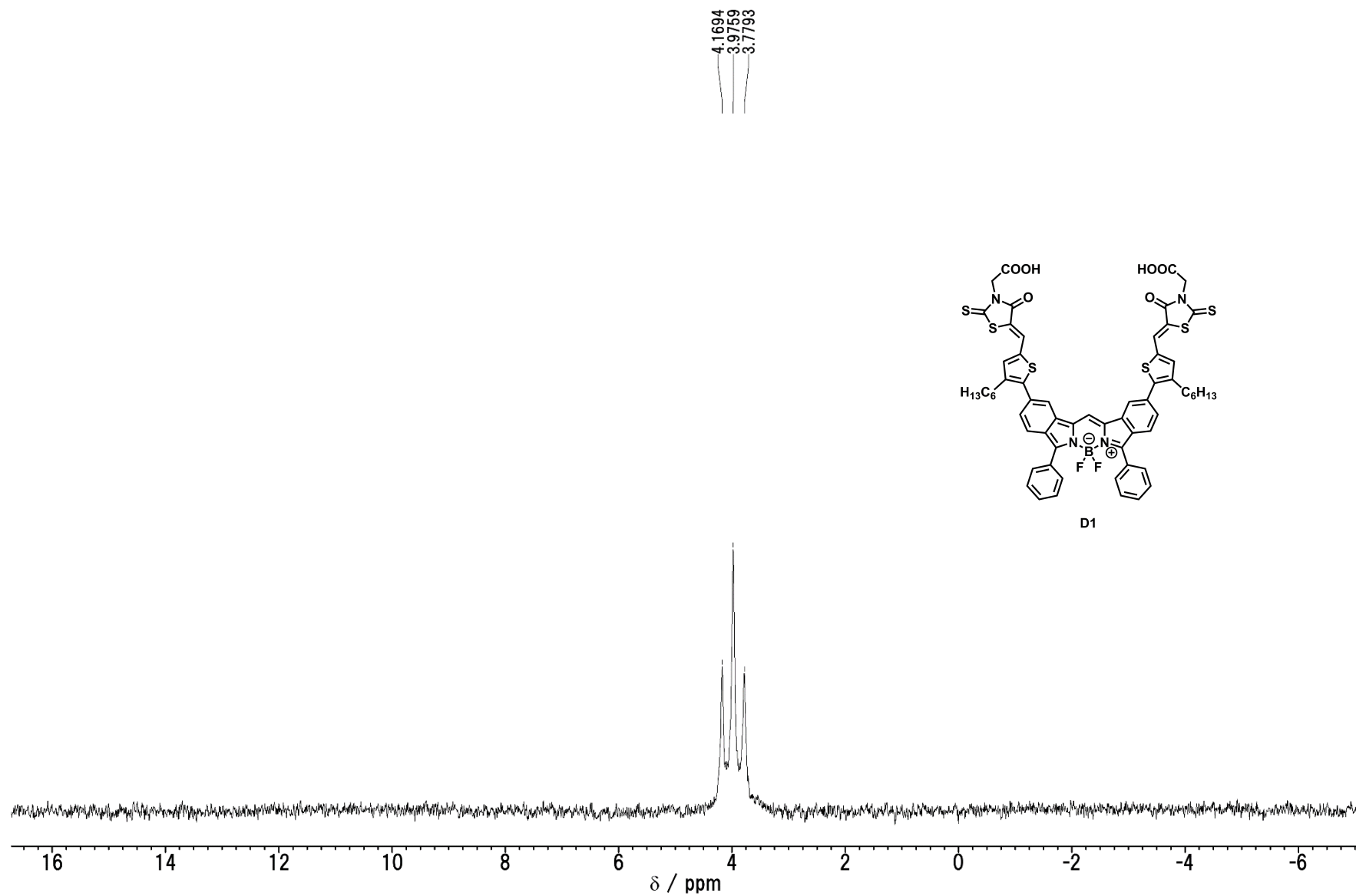


Fig. S13 ^{11}B NMR spectrum of **D1**

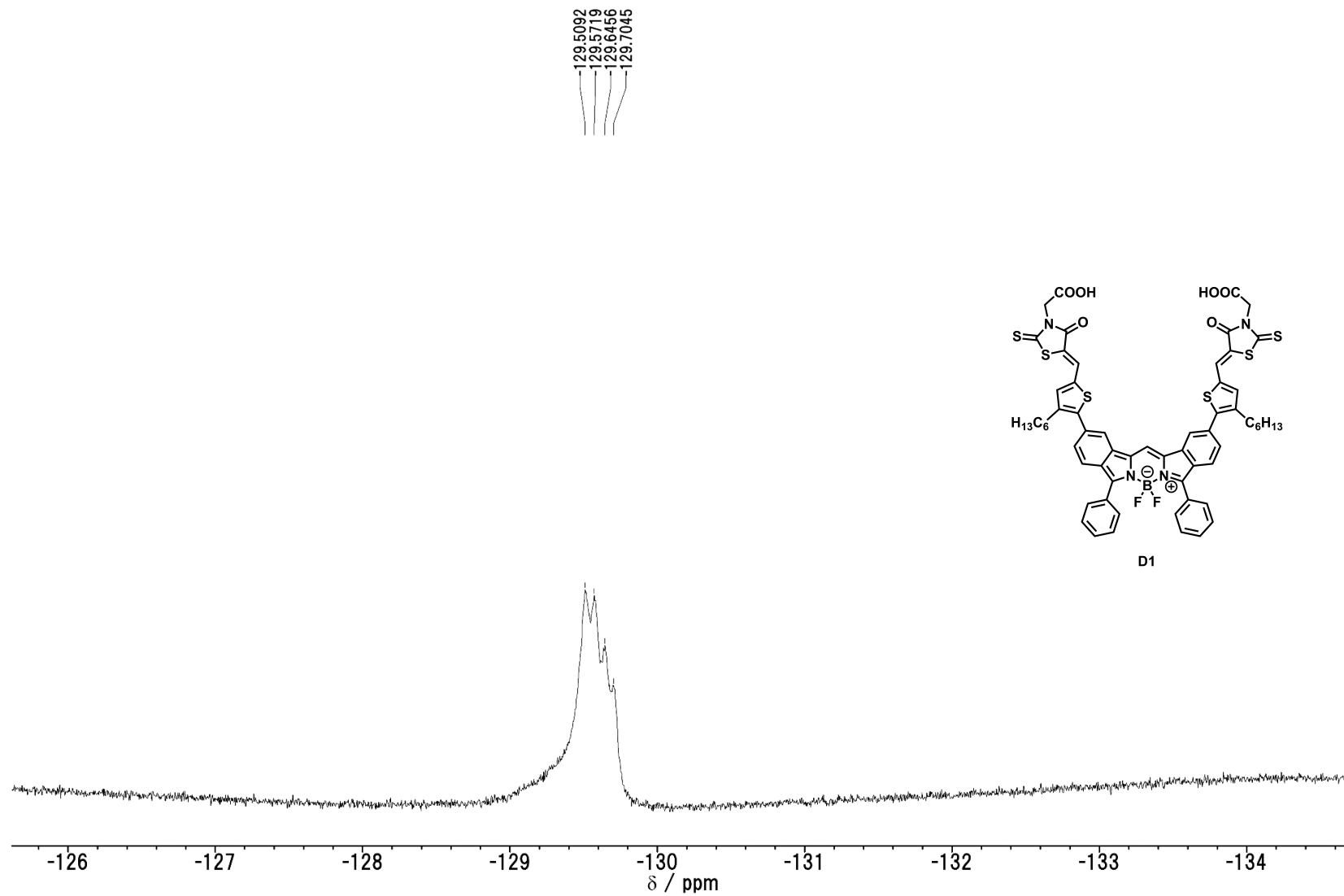


Fig. S14 ¹⁹F NMR spectrum of D1

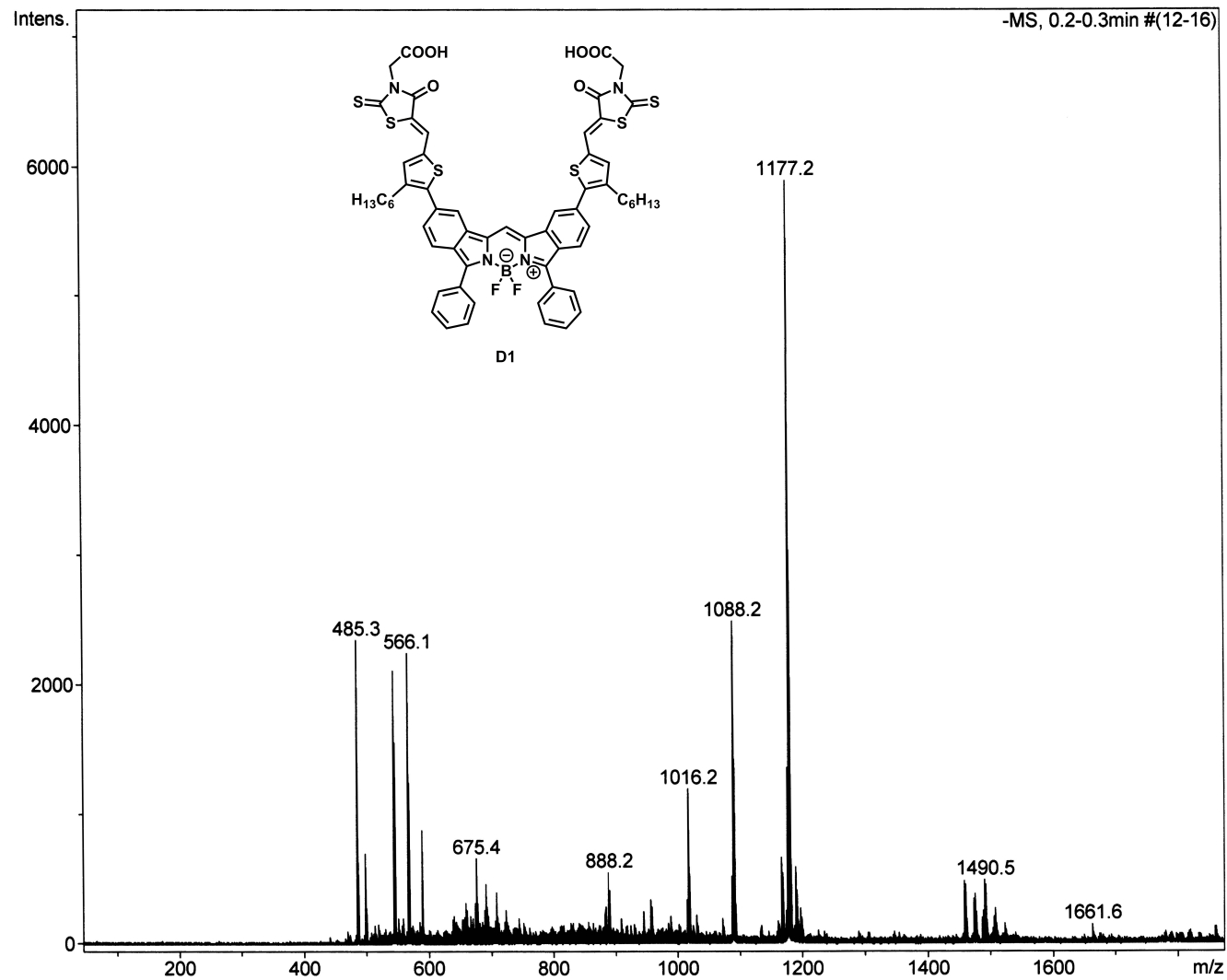


Fig. S15 ESI mass spectrum of **D1**

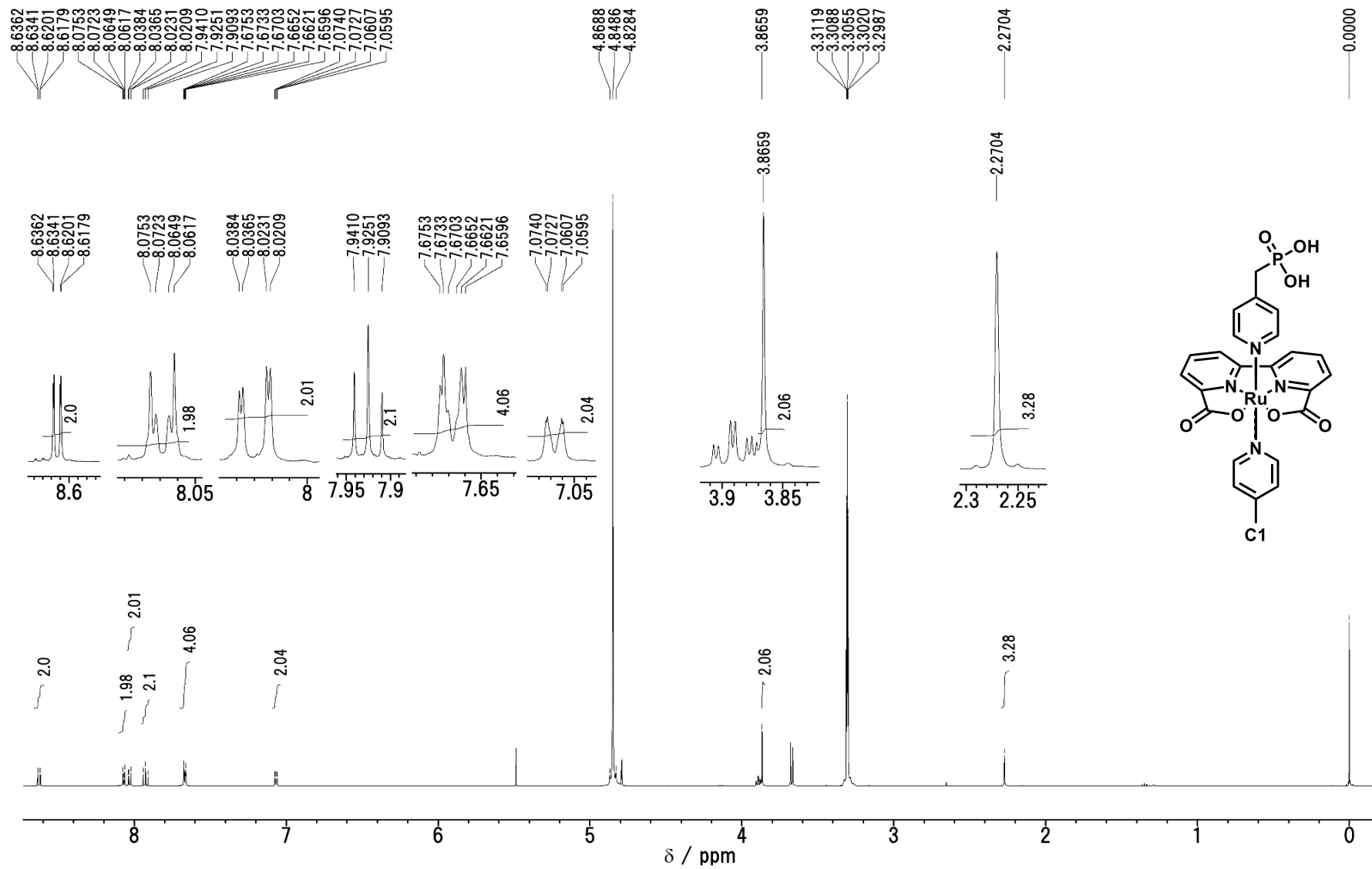


Fig. S16 ^1H NMR spectrum of C1

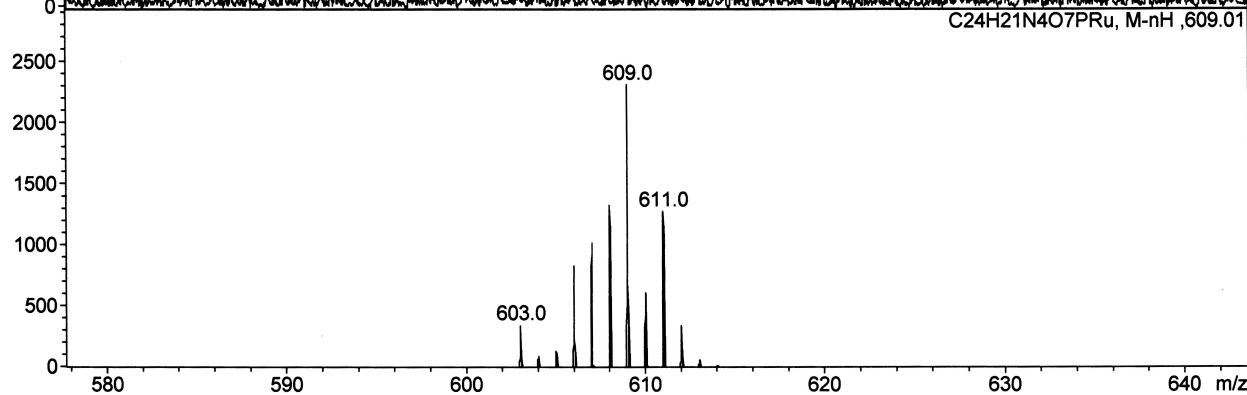
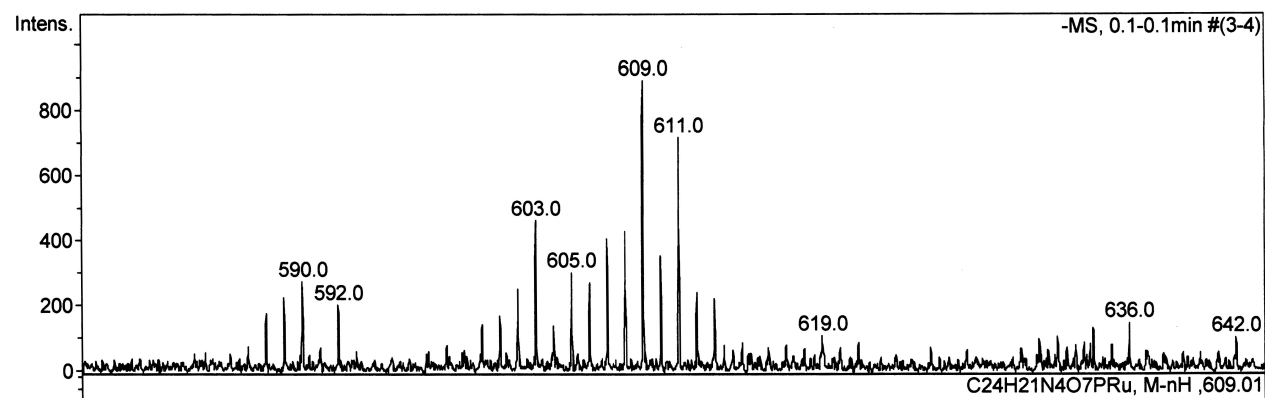
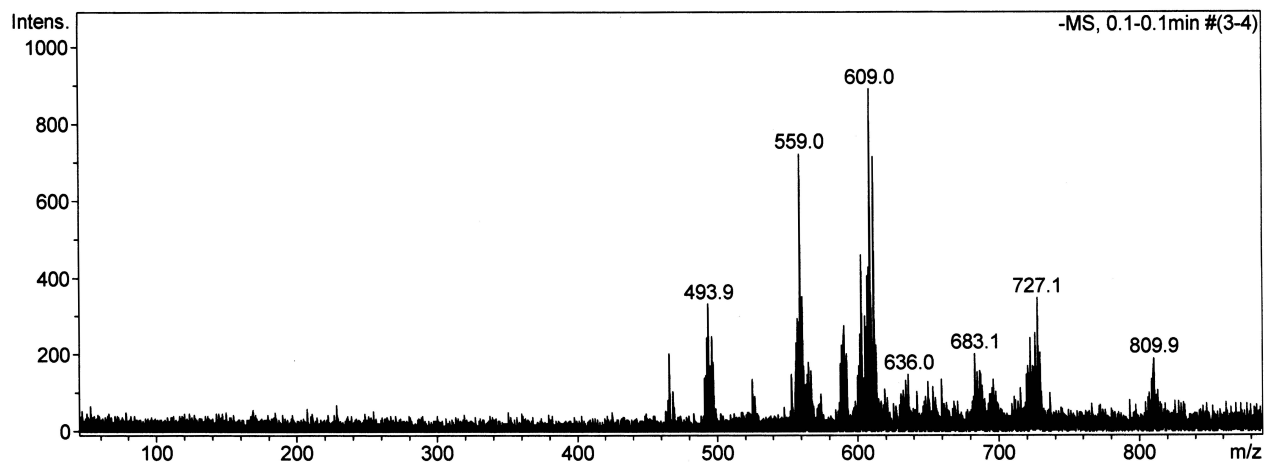


Fig. S17 ESI mass spectrum of C1